JOURNAL OF MATERIALS SCIENCE **39** (2004) 2675–2681

Bipolar electric fatigue behaviour as a function of field strength in antiferroelectric (Pb,Ba,La)(Zr,Sn,Ti)O_3 ceramics

LONGJIE ZHOU, A. ZIMMERMANN*, YU-PING ZENG, F. ALDINGER
Max-Planck-Institut für Metallforschung and Institut für Nichtmetallische Anorganische Materialien, Universität Stuttgart, Pulvermetallurgisches Laboratorium, Heisenbergstrasse 3, 70569 Stuttgart, Germany
E-mail: zhou@mf.mpg.de

The bipolar electric fatigue behaviour of antiferroelectric ceramics with the composition of $Pb_{0.88}Ba_{0.10}La_{0.02}(Zr_{0.55}Sn_{0.35}Ti_{0.10})O_3$ was investigated under various cycling fields. The material exhibits a degradation in the maximum field induced strain, a diffuse AFE-FE phase transition and an enhancement in the diffusion character of the FE-AFE phase transition due to electric cycling. Those variations increase with cycle number, indicating a logarithmic fatigue up to 10^8 cycles. There is no indication for the variations to be recovered, and the symmetry of the negative and positive parts of the strain hysteresis loops still remains. Higher cycling field results in a stronger deterioration of the maximum field induced strain and a larger extent of diffusion in AFE-FE and FE-AFE phase transitions. The normalized maximum strain shows nearly the same scale of degradation when the materials are cycled at various electric fields. After a heat treatment at 500°C for 1 h, the variations in the AFE-FE and FE-AFE phase transition due to cycling disappear, whereas the maximum strain resumes almost to its original value. Electrochemical variations are considered to contribute to the main fatigue mechanism for the material under investigation.

1. Introduction

The aging effect of piezoelectric materials under alternating electric fields, namely degradations in polarization and field induced strain, is called the electric fatigue of the materials, which has been the major hindrance for their applications as non-volatile memory devices and actuators [1]. Intensive investigations have been conducted to reveal the fatigue behaviour and mechanisms of the materials for more than a dozen of years. It has been found that numerous factors, such as composition [2], grain size [3], porosity [1], electrode [4], surface contamination [5], temperature [6], frequency [7], the strength [8] and type [9] of cycling field, exert an influence, more or less, on the fatigue behaviour of piezoelectric bulk materials and thin films. Four stages of electric fatigue in ferroelectrics were explored [10, 11]. During an incubation period up to 10^5 cycles, remnant polarization and coercive field show only minor changes. Between 10^5 to 10^7 cycles, a stage of logarithmic fatigue will be observed, where remnant polarization and coercive field show marked decreases. At the following stage of saturation (10^7 to 10^8 cycles), remnant polarization and coercive field stay almost constant and at the final stage of "rejuvenation" (above 10^8 cycles), the properties recover to some extent. With regard to the mechanisms that cause electric fatigue of piezoelectric materials, there have been numerous models including those of mechanical deterioration and electrochemical variations [12]. The former is based on the idea that microcracks reduce the local effective field or yield conductive corrosion pathways in the material, thus decreasing the number of domains which switch in the proximity of such cracks [13, 14]. The latter is based on the scenario that domains become inactive due to point defects pinning the domain walls [15–17]. The electrochemical variations will be relieved by heat treatment at temperatures exceeding 300 to 500°C [18], while the mechanical deterioration in fatigued samples can not be resumed below sintering temperatures.

The above-mentioned findings on influencing factors of electric fatigue, fatigue stages and fatigue mechanisms are mostly based on the investigation of ferroelectric bulk materials and thin films rather than antiferroelectrics. There are only a few reports on the fatigue in polarization of antiferroelectric bulk materials and thin films [2, 19–22]. So far, no other studies have been performed according to our knowledge on electric fatigue in the field induced longitudinal strain of antiferroelectric materials. The fatigue behaviour of antiferroelectric materials with different compositions and their fatigue

**Present address:* Robert Bosch GmbH, Corporate Research and Development.

mechanisms still remain to be exploited. Furthermore, the influence of cycling fields with different maximum strengths on the fatigue behaviour of antiferroelectric ceramics is unknown. In this paper, we present the investigation of bipolar electric fatigue behaviour in antiferroelectric (Pb,Ba,La)(Zr,Sn,Ti)O_3 ceramics under various cycling fields. The electric fatigue behaviour of the material and the influence of cycling fields on the fatigue will be discussed. The fatigue behaviour and mechanism of this composition will be compared with those of antiferroelectric (Pb,La)(Zr,Sn,Ti)O_3 ceramics.

2. Experimental procedure

2.1. Sample preparation

The composition of the antiferroelectric ceramics investigated in this paper is $Pb_{0.88}Ba_{0.10}La_{0.02}(Zr_{0.55}Sn_{0.35}Ti_{0.10})O_3$. Samples were prepared by solid-state reactions and conventional sintering, using commercially available reagent-grade raw oxides, i.e., PbO, BaO, La_2O_3, ZrO_2, SnO_2 and TiO_2, as starting materials. Firstly, the starting oxides were mixed and attrition milled in isopropanol for 6 h with small zirconia balls as milling media in order to increase their reactivity and to get highly intimately mixed materials. After drying, the mixtures were calcined at 850°C for 5 h and attrition milled again for 6 h. The resulting powders were dried at 60°C for 24 h and cold isostatically pressed at 200 MPa into disks of 14 mm in diameter and 2 mm in thickness. The disks were sintered in an oxygen atmosphere which is necessary to achieve dense samples, using a heating and cooling rate of 3°C/min and a holding time of 2 h at 1150 and 1250°C, respectively. In order to minimise the lead loss during sintering, the samples were heated inside a closed alumina crucible with tablets of a powder mixture of $PbZrO_3$ and 8 mol% ZrO_2, which provides a constant PbO pressure. The sintered samples were ground and fine polished to 1 micron finish into thin discs, about 1.0 mm in thickness, with flat and parallel major surfaces. Finally the samples were ground into round discs with 10 mm in diameter after annealing at 500°C for 8 h in air and sputtering with gold as electrodes on both major surfaces.

2.2. Measurements and cycling

The Rietveld method was used to detect the lattice parameters of the perovskite structures by X-ray diffractometry (Siemens D5000) with scanning steps of 0.008° per second. A refinement programme, WINCELL, was used to refine the lattice parameters. Theoretical densities of the samples were then calculated according to the lattice parameters and the composition of the samples. Density measurements were performed via the Archimedes principle. Fracture surface and polished or polished-etched surfaces of the sintered samples were observed by optical microscopy (Leica DM RM, Leica Microsystems AG, Wetzlar, Germany) and scanning electronic microscopy (SEM, Jeol 6300F). A solution of 5 ml of HCl and 95 ml of distilled water, containing a few drops of HF acid, was used as etchant. A dozen of seconds of exposure gave clear images of the grains. An inductive strain gauge was employed to measure the field induced longitudinal strain of the disc samples immersed in silicone oil to prevent arcing. Sinusoidal fields with a frequency of 0.05 Hz were used for the measurements. Unless specially indicated, the strain referred to in this paper is the longitudinal strain.

The maximum values of the bipolar cycling fields were chosen as 2.1, 2.6 and 3.1 kV/mm, which are 0.5, 1.0 and 1.5 kV/mm higher than the antiferroelectric to ferroelectric transition field (of about 1.6 kV/mm), respectively. An electric transmitter provided the needed sinusoidal voltage (50 Hz) from the normal electric line voltage. Samples were immersed in a bath of silicon oil in order to avoid arcing and to ensure good thermal conductivity. The cycling field was slowly and steadily increased and decreased when loading and unloading. The starting and ending time of cycling were determined as the times when the field strength passed the value of 1.6 kV/mm. After a certain period of cycling, the samples were removed from the cycling set-up for strain hysteresis loop measurements under sinusoidal fields with the same maximum strength as in case of the corresponding cycling fields. It was observed that the strain hysteresis loops in the first few cycles might not be steady. The measurement was conducted till the strain hysteresis loop was stable for 4 cycles, which were used to calculate the average strains and fields to characterize the fatigue behaviour of the materials. Cycling and strain hysteresis loop measurements were repeated till a cycle number larger than 10^8 was reached.

The strain hysteresis loop measurements were conducted again after a heat treatment of the fatigued samples at 500°C for 1 h with a heating rate of 5°C/min and a cooling rate of 3°C/min. The microstructure of the fatigued samples was also observed by optical microscopy after the electrodes had been removed, and by scanning electron microscopy after etching of the surface.

3. Results

3.1. Crystal structure, microstructure, and strain hysteresis loop

The X-ray diffraction pattern of the material shows a single tetragonal crystal structure, indicating an antiferroelectric phase. The refined lattice parameters are $a = 4.111 \pm 0.001$ Å and $c = 4.097 \pm 0.001$ Å, respectively. The specimens, translucent after polishing, were highly densified up to more than 99% of the theoretical X-ray density. As shown in Fig. 1, the grain sizes of the ceramics are fine, with an average about 2 μm. The maximum pore size within the material is less than 5 μm, as observed on the polished surface of the samples. The material with high density and fine grain size is expected to exclude markedly negative influences of large porosity and large grain size on the fatigue behaviour and to exhibit its intrinsic electric fatigue behaviour.

The strain hysteresis loops of virgin samples, with maximum fields of 2.1 and 3.1 kV/mm, are shown in Fig. 2a and b, respectively. The loops are typical

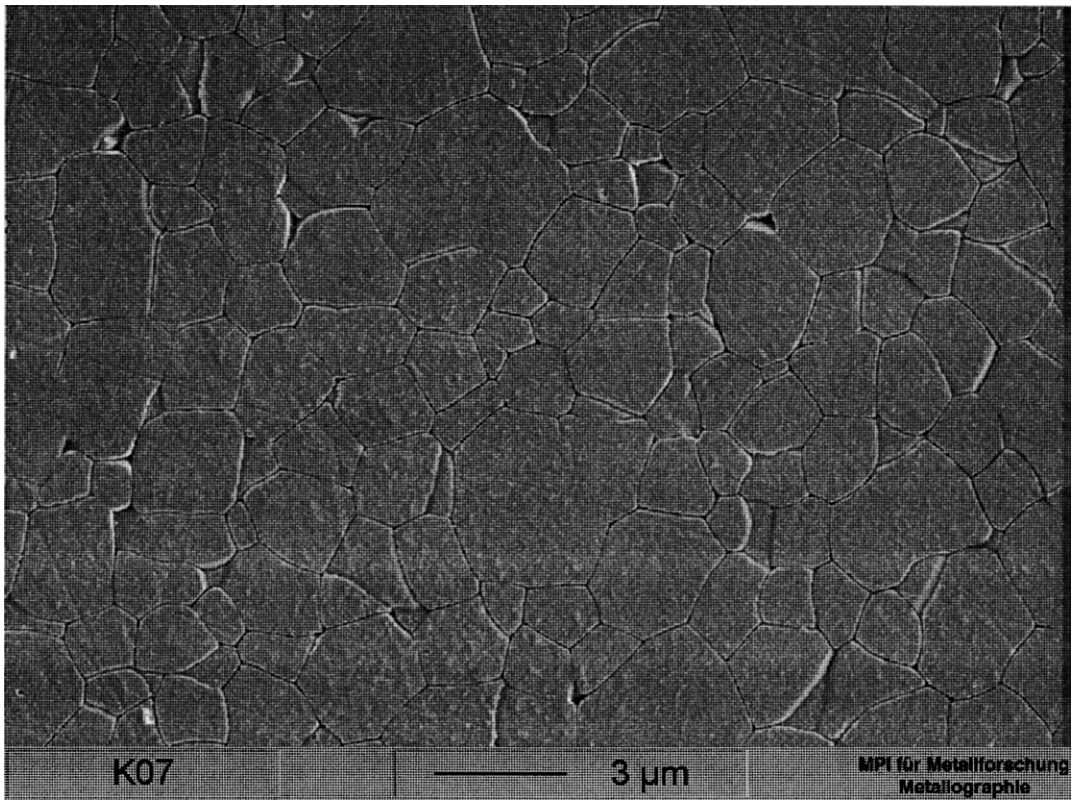

Figure 1 SEM micrograph of the polished-etched surface of the material.

for antiferroelectric materials, with sudden increases in field induced strain due to the antiferroelectric-ferroelectric (AFE-FE) phase transition. The transition field (E_{AF}) is about 1.6 kV/mm, where the field induced strain shows a sudden increase with increasing electric field. The back switching, ferroelectric-antiferroelectric phase transition (FE-AFE), exhibits a diffuse behaviour, with a transition field (E_{FA}) of about 0.5 kV/mm, where the strain exhibits the fastest decrease with decreasing electric field. The diffusion nature of the FE-AFE phase transition is attributed to microstresses in the field forced ferroelectric state due to the field induced strain. The microstresses provide additional energy to some grains, beside the electric field, and cause the grains to undergo phase transition not at exactly the same point but within a range of electric fields. It is found that the measured AFE-FE transition strain (S_T) of the material shows a geometric effect. With the same diameter, thicker disc samples exhibit smaller transition strain, while thinner ones show larger relative deformation. Samples with a thickness of about 1.0 mm display a transition strain of about 0.08%.

3.2. Variations in strain hysteresis loops due to cycling

Fig. 2c to f show strain hysteresis loops of the materials cycled at 2.1 and 3.1 kV/mm for $10^{6.25}$ and 10^8 cycles, respectively. Comparing Fig. 2c and e with 2a and Fig. 2d and 2f with 2b, it is found that the strain hysteresis loop of the material exhibits obvious variations in three aspects due to cycling. Firstly, the maximum strain (S_m) at the maximum field is degraded with increasing cycle number. The maximum strains at 2.1 and 3.1 kV/mm are about 0.11 and 0.14%, respectively. After cycling at 2.1 and 3.1 kV/mm for $10^{6.25}$ cycles, there is only a slight decrease in S_m in both cases, while S_m is decreased to 0.09 and 0.11%, respectively after 10^8 cycles. Secondly, the AFE-FE phase transition becomes more and more diffuse with increasing cycle number. As shown in Fig. 2a and b, the phase transitions of virgin samples exhibit normal behaviour with a clearly defined transition field (1.6 kV/mm) and a sudden increase in strain at this field strength. After cycling for $10^{6.25}$ cycles, it is obvious that the phase transition takes place in a range rather than at a particular electric field. It is clear that the phase transition becomes diffuse towards to low electric fields since the ending field of the phase transition (E_{AFE}) stays nearly constant at E_{AF}. The starting field of the transition (E_{AFS}) shifts more close to zero when the cycle number approaches 10^8. However, the phase transition becomes so diffuse that E_{AFE} is difficult to determine when the cycle number is so large. Finally, the FE-AFE phase transition also becomes more diffuse due to cycling. Actually, the FE-AFE phase transition is diffuse to some extent when the materials are still in the virgin state, as shown in Fig. 2a and b. Due to cycling, the phase transition extends to both lower and higher electric fields. However, the phase transition is so diffuse that it is difficult to decide exactly the starting field and the end fielding of the transition when the cycle number is up to $10^{6.25}$.

As a whole, strain hysteresis loops due to cycling exhibit not only degradation in S_m, but also diffuse nature of the AFE-FE phase transition and an enhancement in diffuse character of FE-AFE phase transition. Those variations increase with increasing cycle number. As a result, both the positive and the negative parts of the

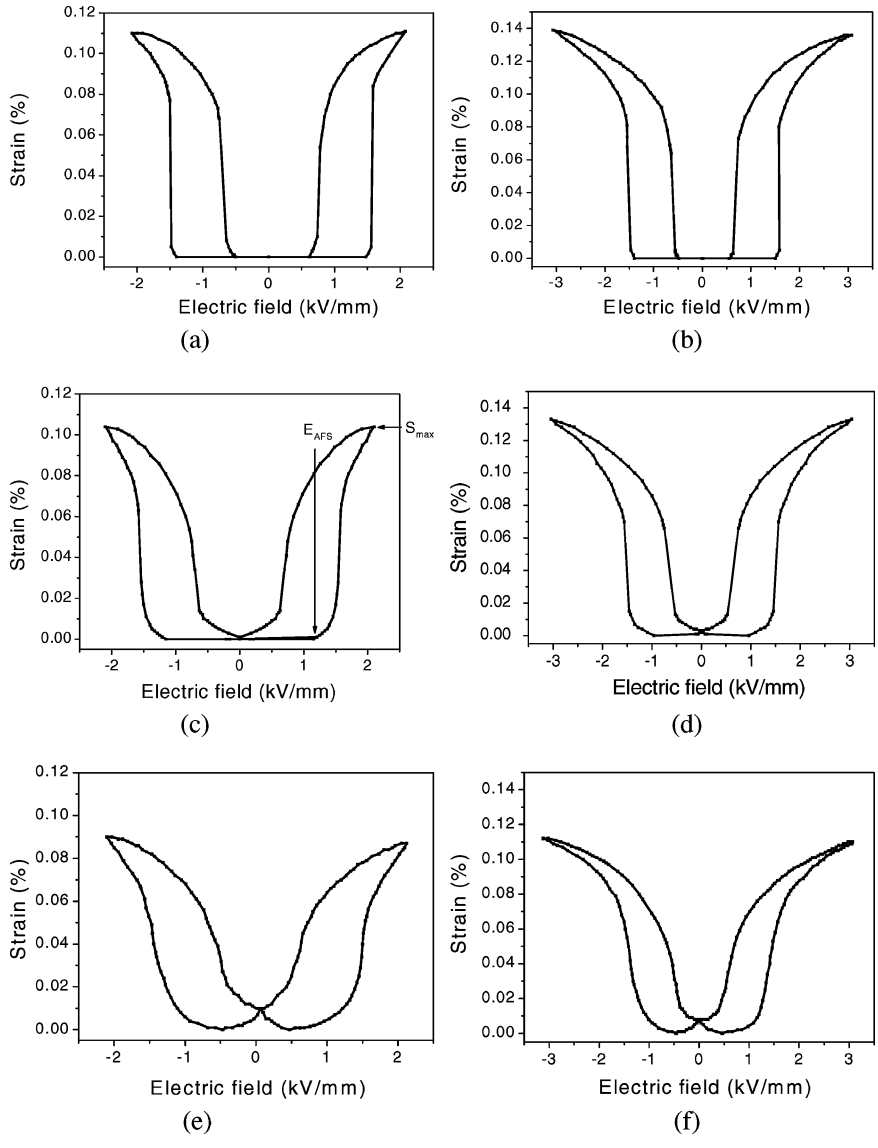

Figure 2 Strain hysteresis loops of samples before and after cycling: (a) At 2.1 kV/mm, virgin state, (b) At 3.1 kV/mm, virgin state, (c) At 2.1 kV/mm, after $10^{6.25}$ cycles, (d) At 3.1 kV/mm, after $10^{6.25}$ cycles, (e) At 2.1 kV/mm, after 10^8 cycles and (f) At 3.1 kV/mm, after 10^8 cycles.

strain hysteresis loop lost their slimness gradually with cycle number. However, the symmetry of the two parts keeps intact during cycling.

3.3. Fatigue behaviour as a function of the strength of the cycling field

Since the starting field of AFE-FE phase transition (E_{AFS}) and the maximum strain (S_m) could be always identified exactly in strain hysteresis loops with cycle numbers from zero up to 10^8, the two parameters are used to characterize the fatigue behaviour of the material. E_{AFS} as a function of cycle number under different cycling fields is shown in Fig. 3a. As a whole, E_{AFS} decreases with cycle number, which indicates that the diffuse character of the AFE-FE phase transition increases with cycle number. E_{AFS} shifts from about 1.6 kV/mm at the first few cycles to about 0.4 kV/mm at 10^8 cycles, with fast variation rate within a range of 10^6 to 10^7 cycles. With increase in the strength of the cycling field, E_{AFS} exhibits a faster decrease rate at cycle numbers lower than 10^6, but shows a slower decrease rate at cycle numbers higher than 10^7. As a result, for a given cycle number, higher cycling fields yield a more diffuse for the AFE-FE phase transition. S_m as a function of cycle number under different cycling fields is shown in Fig. 3b. In general, the material exhibits high fatigue resistance in field induced strain with an onset of degradation in S_m at 10^5 cycles. S_m undergoes logarithmic fatigue after 10^5 cycles and shows no indication of recovery till 10^8 cycles.

Fig. 4 shows the normalized strain S_m as a function of cycle number at various cycling fields. It is found that the normalized S_m follows nearly the same evolution of deterioration with cycle number, independent of the applied cycling fields. Obvious degradation in S_m occurs from 10^5 cycles; after 10^8 cycles, S_m decreases to about 75% of its original values for all cycling fields.

3.4. Microstructure of fatigued samples and recovery of the strain hysteresis loop

No damaged structure was found in the fatigued samples. There are neither macro nor micro-cracks found at the major surface after the electrodes were removed nor

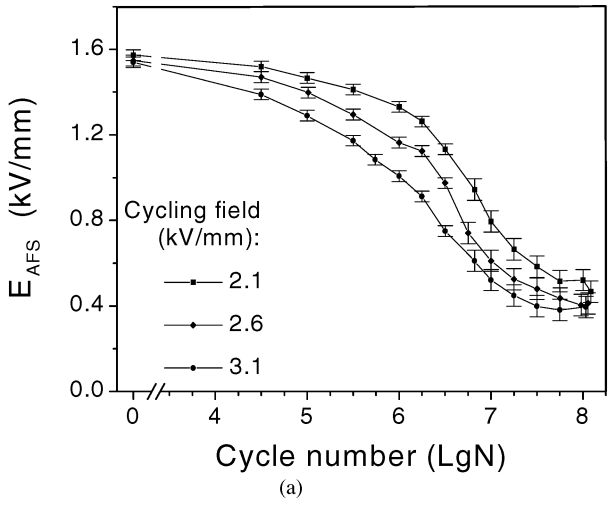

(a)

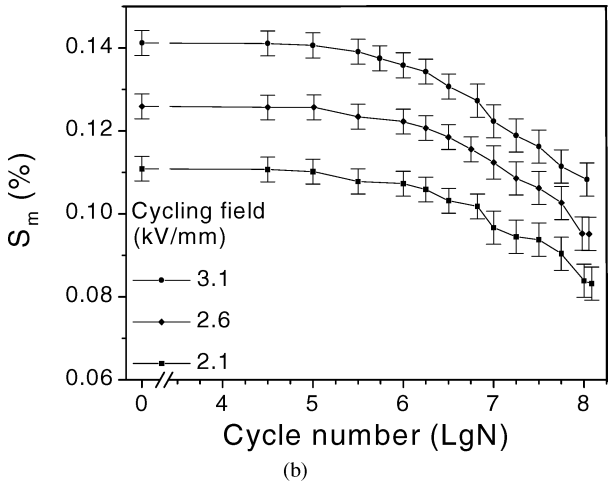

(b)

Figure 3 E_{AFS} and S_m as a function of cycle number at different cycling fields.

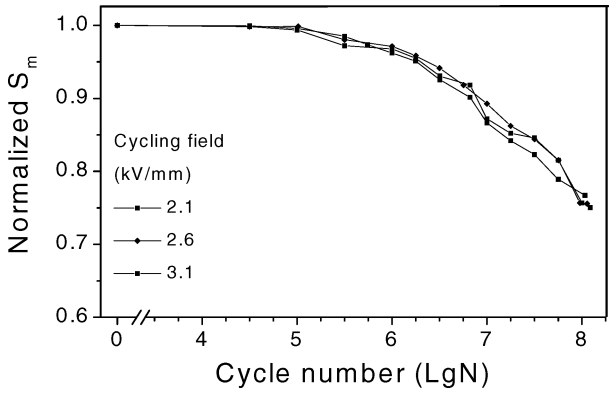

Figure 4 Normalized S_m with cycle number at different cycling fields.

so-called corrosion paths were observed at the etched major surface.

Fig. 5 shows the strain hysteresis loop for the fatigued-recovered state of a sample fatigued by cycling at 3.1 kV/mm for 10^8 cycles and recovered by heat treatment at 500°C for 1 h. The strain hysteresis loop for the virgin state of the sample, shown in Fig. 2b, is also plotted in the Fig. 5 for comparison. Compared with the virgin state, the strain hysteresis loop for the fatigued-recovered state of the sample indicates that field induced strain was nearly fully recovered. The AFE-FE transition field resumed its initial value, while the diffuse character of AFE-FE phase transition due

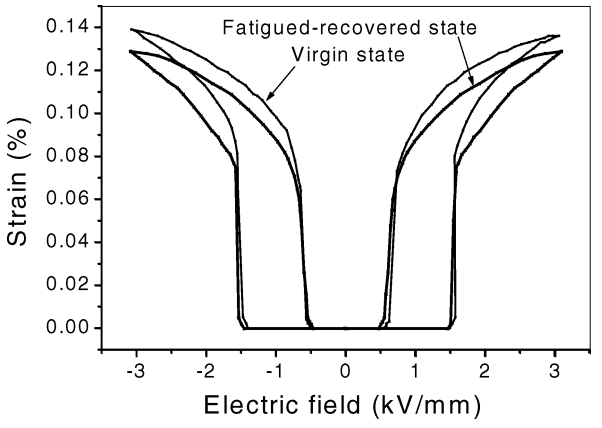

Figure 5 Strain hysteresis loops for virgin and fatigued-recovered states of the material (Fatigued: cycling at 3.1 kV/mm for 10^8 cycles; recovered: heat treatment at 500°C for 1 h).

to cycling disappeared. The FE-AFE phase transition was also almost recovered to its original behaviour. The AFE-FE transition strain and the maximum strain, however, could not be fully resumed to their original values.

4. Discussion

As mentioned in the introduction, the electric fatigue in ferroelectric materials exhibits four stages, including incubation, logarithmic fatigue, saturation and rejuvenation. The remnant polarization and coercive field decrease slightly, undergo logarithmic fatigue, stay almost constant and recover to some extent from the first stage to the final one. Those stages for ferroelectric ceramics are also observed in the maximum field induced strain when cycle number is up to 10^8, where the strain shows some recovery [12]. The stages of electric fatigue for antiferroelectric ceramics have not yet been fully understood, but it is believed that the materials will undergo similar fatigue stages as ferroelectric ones. According to the degradation of S_m, it is assumed that the antiferroelectric fatigue in this study undergoes stages from the incubation to the logarithmic state under all of the cycling fields even though cycle number exceeds 10^8 since there is no indication of recovery of S_m.

In this investigation, the mechanical deterioration as the main source for fatigue can be excluded since no indication of damaged microstructure in the fatigued specimens was found. Furthermore, a rejuvenation of the AFE-FE and FE-AFE transition behaviour as well as a large extent of recovery of the maximum field induced strain was observed after heat treatment of the fatigued samples. Therefore, the electrochemical variations, i.e., the generation, migration and redistribution of some charged species, most probably the oxygen vacancies, is considered to be responsible for to the main fatigue mechanism of the material. The charged defects in the material migrate to the domain wall or grain boundary during the switching of AFE-FE and FE-AFE phase transitions under electric field and are captured by domain walls or grain boundaries or electrode-antiferroelectric interface. With the accumulation of this process, the piled up space charges would pin some domains and, thus, block the further

phase transition and the reorientation of the domains, resulting in the occurrence of degradation in the maximum strain. The massive generation, migration and redistribution of charged defects also leads to residual microstresses, which provide additional energy for the generation and stabilization of the ferroelectric phase. Therefore, the AFE-FE phase transition in some grains occurs at lower field than that needed for normal transition, which contributes to the diffuse character of the AFE-FE phase transition. The stronger stabilization of the ferroelectric phase under residual microstresses is assumed to be the source of the diffuse nature of the AFE-FE phase transition and the enhancement in diffuse character of the FE-AFE phase transition. The majority of the charged species, most probably oxygen vacancies, are reduced and redistributed by the heat treatment, thus, the material is recovered to a great extent to its original states.

It is reported that the degradation of properties, including polarization and strain, is strongly related to the cycling field in PZT ferroelectric bulk materials [12]. As for the antiferroelectric ceramics investigated in this study, it is also found that higher cycling fields result in stronger degradation in the maximum field induced strain and larger extent of diffuse character of AFE-FE and FE-AFE phase transitions, which indicates that higher electric fields enhances the generation, migration and redistribution of charged species and thus result in a stronger fatigue effect.

Compared with the antiferroelectric ceramics ($Pb_{0.97}La_{0.02}(Zr_{0.77}Sn_{0.14}Ti_{0.09})O_3$) investigated previously [23], the ceramics in the present study exhibit a distinct electric fatigue behaviour and mechanism. The former shows no diffuse AFE-FE phase transition due to cycling, but exhibits a damaged microstructure with dendritic macrocracks and microcrack clouds after high cycle numbers. The fatigue mechanism of the materials is attributed to the combination of both mechanical deterioration and electrochemical variations. The latter displays a diffuse AFE-FE phase transition from the beginning of the fatigue and no indication of damaged microstructure when the cycle number exceeds 10^8. Electrochemical variations due to cycling mainly contribute to the fatigue behaviour of the ceramics. It is concluded that fatigue behaviour and mechanism of antiferroelectric ceramics depend strongly on the composition of the materials, which is assumed to result from the differences in the properties of the ceramics. The $(Pb,La)(Zr,Sn,Ti)O_3$ antiferroelectrics need high energy, i.e., high electric field (3.9 kV/mm) for the AFE-FE phase transition and show a large transition strain of about 0.26%, while the $(Pb,Ba,La)(Zr,Sn,Ti)O_3$ materials undergo the AFE-FE phase transition at low exciting energy, namely low electric field (1.6 kV/mm), and exhibit a small transition strain of 0.08%. The large transition strain, yielding large microstresses in the material, is considered as the main cause of damaged microstructure in the former case, whereas the small energy gap between antiferroelectric and ferroelectric states in the latter material makes it easy to yield diffuse AFE-FE transition under cycling induced residual microstresses in the material.

5. Conclusions

Based on the above investigation, the following conclusions can be drawn on the fatigue behaviour and mechanism of the antiferroelectric material under various bipolar cycling fields:

1. The antiferroelectric material exhibits a number of variations in strain hysteresis loop, including degradation of the maximum field induced strain, diffuse AFE-FE phase transition and an enhancement of diffuse character the FE-AFE phase transition due to bipolar electric cycling.
2. The variations increase with cycle number, indicating a logarithmic fatigue up to 10^8 cycles, without any indication for the variations to be recovered. The symmetry of the negative and positive parts in strain hysteresis loops still stays intact.
3. High cycling fields result in a stronger fatigue effect, namely more pronounced deterioration of the maximum strain and more diffuse AFE-FE and FE-AFE phase transitions.
4. The electrochemical variation, i.e., the generation, migration and redistribution of charged species, most probably the oxygen vacancies, is believed to be the main fatigue mechanism for the material under investigation.

Acknowledgements

The authors gratefully acknowledge financial support by the Deutsche Forschungsgemeinschaft. Mr. Mager's help in technical support is cordially appreciated.

References

1. Q. Y. JIANG and L. E. CROSS, *J. Mater. Sci.* **28** (1993) 4536.
2. Q. JIANG, E. C. SUBBARAO and L. E. CROSS, *J. Appl. Phys.* **75** (1994) 7433.
3. L. E. CROSS and Q. JIANG, *J. Intell. Mater. Syst. Struct.* **35** (1992) 58.
4. W. FAN and S. LEPPAVUORI, *J. Appl. Phys.* **82** (1997) 1293.
5. Q. JIANG, W. CAO and L. E. CROSS, ISAF '92, in Proceedings of the Eighth IEEE International Symposium on Applications of Ferroelectrics (Cat. No. 92CH3080-9) (IEEE, New York, 1992) p. 107.
6. D. WANG, Y. FOTINICH and G. P. CARMAN, *J. Appl. Phys.* **83** (1998) 5342.
7. N. ZHANG, L. LI, J. QI and Z. GUI, *Ferroelectr.* **259** (2001) 109.
8. H. WEITZING, G. A. SCHNEIDER, J. STEFFENS, M. HAMMER and M. J. HOFFMANN, *J. Eur. Ceram. Soc.* **19** (1999) 1333.
9. W. PAN, C. YUE and O. TOSYALI, *J. Amer. Ceram. Soc.* **75** (1992) 1534.
10. C. Z. PAWLACZYK, A. K. TAGANTSEV, K. BROOKS, I. M. REANEY, R. KLISSURSKA and N. SETTER, *Integr. Ferroelectr.* **8** (1995) 283.
11. E. L. COLLA, A. K. TAGANTSEV, D. V. TAYLOR and A. L. KHOLIN, *ibid.* **18** (1997) 19.
12. J. NUFFER, D. C. LUPASCU and J. RÖDEL, *Acta Mater.* **48** (2000) 3783.
13. Q. JIANG, W. CAO and L. E. CROSS, *J. Amer. Ceram. Soc.* **77** (1994) 211.
14. H. M. DUIKER, P. D. BEALE, J. F. SCOTT, C. A. PAZ DE ARAUJO, B. M. MILNICK, J. D. CUCHIARO and L. D. MCMILLAN, *J. Appl. Phys.* **68** (1990) 5783.
15. U. ROBELS, L. SCHNEIDER-STÖRMANN and G. ARLT, *Ferroelectr.* **168** (1995) 301.

16. C. BRENNAN, *ibid.* **150** (1993) 199.
17. A. K. TAGANTSEV and I. A. STOLICHNOV, *Appl. Phys. Lett.* **74** (1999) 1326.
18. J. NUFFER, D. C. LUPASCU and J. RÖDEL, *ibid.* **80** (2002) 1049.
19. W. PAN, Q. ZHANG, A. BHALLA and L. E. CROSS, *J. Amer. Ceram. Soc.* **72** (1989) 571.
20. W. Y. PAN, C. O. DAM, Q. M. ZHANGAND and L. E. CROSS, *J. Appl. Phys.* **66** (1989) 6014.
21. J. H. JANG and K. H. YOON, *Jpn. J. Appl. Phys.* **375** (1998) 162.
22. I. KIM, S. BAE, K. KIM, H. KIM, J. LEE, J. JEONG and K. YAMAKAWA, *J. Korean Phys. Soc.* **33** (1998) 180.
23. L. ZHOU, A. ZIMMERMANN, Y. ZENG and F. ALDINGER, to be published in *J. Amer. Ceram. Soc.*

Received 20 August
and accepted 30 December 2003